

## Photoinactivation of *S. Aureus* by Cationic *meso*-Arylporphyrin and Its Zn(II) Complex

Inga O. Savelyeva,<sup>a</sup> Yulia S. Bortnevskaia,<sup>a</sup> Alexey Yu. Usanov,<sup>a</sup> Natal'ya A. Bragina, Andrey F. Mironov,<sup>a</sup> Anastasia A. Ignatova,<sup>b</sup> Alexey V. Feofanov,<sup>b,c</sup> and Kseniya A. Zhdanova<sup>a@</sup>

<sup>a</sup>MIREA – Russian Technological University, 119571 Moscow, Russian Federation

<sup>b</sup>Shemyakin and Ovchinnikov Institute of Bioorganic Chemistry, Russian Academy of Sciences, 117997 Moscow, Russian Federation

<sup>c</sup>Biological Faculty, Lomonosov Moscow State University, 119992 Moscow, Russian Federation

@Corresponding author E-mail: [zhdanova\\_k@mirea.ru](mailto:zhdanova_k@mirea.ru)

*In this work, cationic meso-arylsubstituted porphyrin and its Zn(II) complex were synthesized. The compounds were characterized by multinuclear NMR spectroscopy, electronic spectroscopy and ESI-mass spectrometry. The photodynamic activity of the porphyrins was studied in relation to S. aureus bacteria and their biofilms. Application of polymeric micelles of Pluronic F-127 as nanosized delivery vehicles supports high antimicrobial photodynamic activity of the synthesized porphyrins. The influence of the central metal atom on the dark and light-induced toxicity of the synthesized compounds was revealed.*

**Keywords:** Synthesis, cationic *meso*-arylporphyrins, photodynamic therapy, Zn(II) complexes, photoinactivation, bacteria, Pluronic F-127.

## Фотоинактивация *S. Aureus* катионным мезо–арилпорфирином и его Zn(II) комплексом

И. О. Савельева,<sup>a</sup> Ю. С. Бортневская,<sup>a</sup> А. Ю. Усанов,<sup>a</sup> Н. А. Брагина,<sup>a</sup> А. А. Игнатова,<sup>b</sup> А. В. Феофанов,<sup>b,c</sup> К. А. Жданова<sup>a@</sup>

<sup>a</sup>МИРЭА - Российский технологический университет, 119571 Москва, Российская Федерация

<sup>b</sup>Институт биоорганической химии им. академиков М.М. Шемякина и Ю.А. Овчинникова РАН, 117997 Москва, Российская Федерация

<sup>c</sup>Биологический факультет, Московский государственный университет им. М.В. Ломоносова, 119992 Москва, Российская Федерация

@E-mail: [zhdanova\\_k@mirea.ru](mailto:zhdanova_k@mirea.ru)

*В работе получены катионные мезо-арилзамещенный порфирин и его комплекс с цинком. Соединения были охарактеризованы методами мультijядерной спектроскопии ЯМР, УФ спектроскопии, ESI масс-спектрометрии. Была изучена фотодинамическая активность порфиринов по отношению к бактериям S. aureus и их биопленкам. В качестве наноразмерных средств доставки фотосенсибилизаторов были использованы полимерные мицеллы Плуороника F-127. Использование Плуороника F-127 значительно увеличило фотодинамическую активность порфиринов. Установлено влияние центрального атома металла на темновую и светоиндуцированную токсичность полученных фотосенсибилизаторов.*

**Ключевые слова:** Синтез, катионные мезо-арилпорфирины, фотодинамическая терапия (ФДТ), Zn(II) комплексы, фотоинактивация, бактерии, Плуороник F-127.

## Introduction

At present, infectious diseases are one of the main problems worldwide and the second leading cause of death.<sup>[1]</sup> Antibiotic's overuse and misprescription have led to the emergence of the antibiotic-resistant pathogen that cannot be effectively treated by the standard therapeutic methods. In this regard, alternative methods of treating infectious diseases are required. Antimicrobial photodynamic therapy (APDT) is one of such methods. APDT is based on the cytotoxic action of reactive oxygen species (ROS) generated by a photoactive substance – photosensitizer (PS) upon excitation by the light.<sup>[2–3]</sup> This technology, with its multi-target action and ability to overcome drug resistance in microorganisms, is effective against gram-positive and gram-negative bacteria, viruses, and fungi.<sup>[4–5]</sup> The PS is a key component in APDT; therefore, the search for effective PS is one of the ways to increase the effectiveness of this method.

Synthetic porphyrins and their metal complexes are in demand today in various fields of technology and medicine.<sup>[6]</sup> Porphyrins are widely used in photovoltaics, microelectronics, catalysis,<sup>[7–9]</sup> and as analytical probes.<sup>[10]</sup> The unique structure of these compounds can be chemically modified to provide the necessary physicochemical properties.<sup>[11–12]</sup> However, medicinal application of the porphyrins is of most significant interest, especially as cytotoxic agents.<sup>[13,14]</sup> Previously, the effectiveness of natural and synthetic porphyrins as PSs in APDT against a wide range of pathogenic microorganisms, such as viruses, bacteria, yeast, and protozoa, was shown.<sup>[15–19]</sup> Cationic derivatives of porphyrins are of particular interest due to the active interaction with the bacterial cell wall.<sup>[20]</sup> It was found that the presence of a zinc(II) ion in the macrocycle promotes intersystem crossing of excited molecules to the triplet state through heavy atom effect, thus enhancing the formation of singlet oxygen.<sup>[21]</sup> Previously, the cationic porphyrin's effectiveness was shown against gram-negative and gram-positive bacteria compared to the anionic or neutral PS. In this regard, we synthesized new symmetric cationic porphyrins with terminal pyridinium groups on short alkyl spacers and their complexes with Zn(II). Antibacterial properties of the synthesized compounds in relation to *S. aureus* suspensions and biofilms were investigated. Pluronic F-127 micelles were used to support PS photodynamic activity.

## Experimental

### General

All chemicals were of analytical grade and purchased from Sigma-Aldrich. The solvents were purified according to standard procedures. NMR (<sup>1</sup>H and <sup>13</sup>C) spectra of the studied solutions in CDCl<sub>3</sub> or (CD<sub>3</sub>OD) were recorded on a Bruker MSL-300 pulse Fourier transform spectrometer. Tetramethylsilane or boron trifluoride etherate was used as an external standard. Elemental analysis was performed on a C, H, N, S analyzer FLASH EA 112 from Termo Finnigan (Italy). Mass spectra were recorded using an 1100 LCMSD liquid chromatograph (Agilent Technologies,

USA) equipped with a mass spectrometric detector with chemical ionization at atmospheric pressure (APCI) and equipped with a UV spectrophotometric detector (DAD). Electronic absorption spectra (EAS) of porphyrin solutions were recorded on a HACH DR-4000V instrument (Hach-Lange, USA) in the wavelength range of 320–1100 nm with a step of 1 nm in quartz cells with an optical path length of 10 mm at room temperature. Stationary emission spectra were recorded using a Perkin Elmer LS-50 luminescence spectrometer (USA) under similar conditions. The values of the fluorescence quantum yield  $\Phi_F$  for the porphyrin free bases and their zinc complexes in DMSO were calculated according to the standard procedure<sup>[22, 23]</sup> using TPP ( $\Phi_F = 0.11$ ) and ZnTPP ( $\Phi_F = 0.033$ ) as standards, respectively.<sup>[24–25]</sup>

### Synthesis

*5,10,15,20-Tetrakis(4-(3-bromopropanoyl)oxyphenyl)porphyrin (1a)*. Pyrrole 0.1 g (1.42 mmol) and 4-(3-bromopropanoyloxy)benzaldehyde 0.38 g (1.50 mmol) were dissolved in chloroform (100 mL). The reaction mixture was saturated with argon and stirred at room temperature for 5 min, then 20  $\mu$ L (0.15 mmol) of boron trifluoride etherate and 200  $\mu$ L of absolute ethanol were added. The reaction mass was stirred under inert atmosphere at room temperature for 2 h. After that, argon was removed and 0.3 g of DDQ (1.35 mmol) was added, resulting mixture was stirred at room temperature for 4 h. The reaction mixture was concentrated under reduced pressure. Oligomeric products were separated by flash chromatography on silica gel G 60, eluted with chloroform. The target product was purified by column chromatography on silica gel G 60, eluted with a system of chloroform:hexane = 4:1. Yield 0.13 g (29 %).  $R_f$  0.5 (CH<sub>2</sub>Cl<sub>2</sub>). EAS (CH<sub>2</sub>Cl<sub>2</sub>)  $\lambda_{max}$  nm (lg $\epsilon$ ): 417 (5.5); 515.5 (4.17); 550.8 (3.78); 590.1 (3.54); 646.5 (3.47). <sup>1</sup>H NMR (CDCl<sub>3</sub>)  $\delta_H$  ppm: –2.74 (2H, c, NH-pyrrole), 3.38 (8H, t,  $J=6.65$  Hz, OCOCH<sub>2</sub>CH<sub>2</sub>Br), 3.86 (8H, t,  $J=6.69$  Hz, OCOCH<sub>2</sub>CH<sub>2</sub>Br), 7.57 (8H, d,  $J=8.34$  Hz, 3,5-(ArH)), 8.30 (8H, d,  $J=8.30$  Hz, 2,6-(ArH)), 8.95 (8H, s, CH-pyrrole). Elemental analysis: found, %: C 56.18; H 3.25; N 4.75. C<sub>56</sub>H<sub>42</sub>N<sub>4</sub>O<sub>8</sub>Br<sub>4</sub>; calculated, %: C 55.20; H 3.47; N 4.60.

*5,10,15,20-Tetrakis(4-(3-bromopropanoyl)oxyphenyl)porphyrinatozinc (1b)*. To 20 mg (0.016 mmol) of **1a** in 10 mL of chloroform, 35 mg (0.16 mmol) of zinc acetate in methanol was added, the mixture was stirred for 3 h. The completion of the reaction was judged by EAS data. The reaction mixture was concentrated in a vacuum, the residue was dissolved in chloroform, and filtered to remove inorganic salts. The target product was purified by column chromatography on silica gel G 60, eluted with methylene chloride/hexane (2:1). Yield 18 mg (90 %).  $R_f$  0.5 (CH<sub>2</sub>Cl<sub>2</sub>). EAS (CH<sub>2</sub>Cl<sub>2</sub>)  $\lambda_{max}$  nm (lg $\epsilon$ ): 419 (5.29), 552 (3.68), 593 (3.2). <sup>1</sup>H NMR (CDCl<sub>3</sub>)  $\delta_H$  ppm: 3.39 (8H, m, CH<sub>2</sub>CH<sub>2</sub>Br), 3.86 (8H, t,  $J = 6.66$  Hz, CH<sub>2</sub>CH<sub>2</sub>Br), 7.60 (8H, d,  $J=8.46$  Hz, 3,5-(ArH)), 8.29 (8H, d,  $J = 8.44$  Hz, 2,6-(ArH)), 8.9 (8H, s, CH pyrrole). Elemental analysis: found, %: C 56.64; H 4.51; N 3.95. C<sub>68</sub>H<sub>64</sub>N<sub>4</sub>O<sub>8</sub>Br<sub>4</sub>Zn; calculated, %: C 58.89; H 4.80; N 4.04.

*5,10,15,20-Tetrakis(4-(3-pyridyl-*n*-propanoyl)oxyphenyl)porphyrin tetrabromide (2a)*. The initial porphyrin **1a** (0.05 g, 0.041 mmol) was dissolved in dry pyridine and boiled for 3 h. The formed precipitate was filtered and washed with chloroform; the solvent was removed under reduced pressure. The reaction product was isolated by recrystallization from diethyl ether. Yield: 58 mg (92 %).  $R_f$  0.2 (CH<sub>2</sub>Cl<sub>2</sub>:EtOAc = 1:1). EAS (CH<sub>3</sub>OH)  $\lambda_{max}$  nm (lg $\epsilon$ ): 415.5 (5.49); 512.5 (4.23); 547.5 (3.83); 589 (3.56); 645.5 (3.54). <sup>1</sup>H NMR (CD<sub>3</sub>OD)  $\delta_H$  ppm: 3.68 (8H, t,  $J = 6.16$  Hz, OCOCH<sub>2</sub>), 5.15 (8H, t,  $J = 6$  Hz, CH<sub>2</sub>CH<sub>2</sub>Py), 7.35 (8H, d,  $J = 8.13$  Hz, 3,5-(ArH)), 7.94 (8H, d,  $J = 8$  Hz, 2,6-(ArH)), 8.19 (8H, t,  $J = 7.72$  Hz, 3,5-Py), 8.59–8.69 (12H, m, 4-Py+CH pyrrole), 9.25 (8H, d,  $J = 5.66$  Hz, 2,6-Py). <sup>13</sup>C NMR (CD<sub>3</sub>OD)  $\delta_C$  ppm: 171.36, 150.69, 145.80, 144.74, 139.38, 134.97, 128.33, 119.62, 119.19, 60.74, 30.16, 26.12. Elemen-

tal analysis: found, %: C 60.98; H 4.13; N 7.09,  $C_{76}H_{62}N_8O_8Br_4$  calculated, %: C 59.47; H 4.07; N 7.30. LCMS (ESI)  $m/z$ : 302.1 [ $M^+ - 4Br^-$ ]; the molecular formula of  $C_{76}H_{62}N_8O_8$  requires 303.6.

*5,10,15,20-Tetrakis(4-(3-pyridyl-n-propanoyl)oxyphenyl)porphyrin tetrabromide zinc complex (2b)*. 0.05 g (0.039 mmol) of porphyrin **1b** was dissolved in 5 mL of dry pyridine and boiled during 3 h. The formed precipitate was filtered and washed with chloroform; the solvent was removed under reduced pressure. The reaction product was isolated by recrystallization from diethyl ether. Yield 43 mg (70 %).  $R_f$  0.45 (CH<sub>3</sub>OH).  $R_f$  0.2 (CH<sub>2</sub>Cl<sub>2</sub>:EtOAc=1:1). EAS (CH<sub>3</sub>OH)  $\lambda_{max}$  nm (lg $\epsilon$ ): 428 (5.35); 561 (4.15); 601 (3.85). <sup>1</sup>H NMR (CD<sub>3</sub>OD)  $\delta_H$  ppm: 3.68 (8H, t,  $J = 6.16$  Hz, OCOCH<sub>2</sub>), 5.15 (8H, t,  $J = 6$  Hz, CH<sub>2</sub>CH<sub>2</sub>Py), 7.35 (8H, d,  $J = 8.13$  Hz, 3,5-(ArH)), 7.94 (8H, d,  $J = 8$  Hz, 2,6-(ArH)), 8.19 (8H, t,  $J = 7.72$  Hz, 3,5-Py), 8.59–8.69 (12H, m, 4-Py+CH pyrrole), 9.25 (8H, d,  $J = 5.66$  Hz, 2,6-Py). <sup>13</sup>C NMR (CD<sub>3</sub>OD)  $\delta_C$  ppm: 171.36, 150.69, 145.80, 144.74, 139.38, 134.97, 128.33, 119.62, 119.19, 60.74, 30.16, 26.12. Elemental analysis: found, %: C 60.98; H 4.13; N 7.09,  $C_{76}H_{62}N_8O_8Br_4$  calculated %: C 59.47; H 4.07; N 7.30.

### Photodynamic Activity

*Partition coefficients of 1-n-octanol/water.* Partition coefficients of compounds **2a,b** were measured using 1-*n*-octanol and aqueous phosphate-buffered saline (PBS) by the described method.<sup>[26]</sup> Porphyrins (1.0–1.5 mg) were dissolved in 3 mL of 1-*n*-octanol, previously saturated with a PBS solution. The same volume of PBS saturated with 1-*n*-octanol was added, sonicated for 30 min and stirred at room temperature for 30 min. The organic and aqueous phases were separated by centrifugation. The distribution coefficients were calculated as the ratio between the absorption of the Soret band of photosensitizers in the organic ( $A(org)$ ) and aqueous phases ( $A(aq)$ ) and the dilution coefficients for the organic ( $d(org)$ ) and aqueous ( $d(aq)$ ) layers in accordance within the above way:

$$P = \frac{A(org) \cdot d(org)}{A(aq) \cdot d(aq)}$$

*Cells and culture conditions.* Bacteria (*Staphylococcus aureus* 209P) were cultured in a liquid medium (Mueller-Hinton: dry beef broth extract 4 g/L, starch 1.5 g/L, casein hydrolyzate 17.5 g/L) at 37 °C, 100 % humidity and gentle mixing.<sup>[27]</sup> Antimicrobial activity of PSSs was characterized by the minimal inhibitory concentrations (MICs), *i.e.* the minimal PS concentration causing total inhibition of bacterial growth. MICs were determined using a twofold microtiter broth dilution assay in 96-well plates. Mid-log phase cultures were diluted to  $(0.75 \pm 0.25) \cdot 10^4$  CFU/mL. The concentration of PSSs varied from 0.3 to 20  $\mu$ M. A probe volume was 100  $\mu$ L. The study of antibacterial activity was performed in 3 repetitions for **2a,b** compounds, the result was averaged. The cells were irradiated for 15 min using a halogen lamp (500 W) with a light dose of 128 J/cm<sup>2</sup>. The growth inhibition was calculated by measuring the optical density in each well at a wavelength of 595 nm after 20 h of cells incubation with compounds **2a,b**. The same procedures were performed for non-irradiated control plates.

*Biofilms.* For biofilm formation overnight culture of *S. aureus* was diluted to 10<sup>7</sup> CFU/mL into fresh Mueller–Hinton broth and grown for 20 h at 37 °C in the wells of 96-well flat-bottom plates. Then the plate was washed twice with PBS to remove bacteria in suspensions, the compounds **2a,b** were added to the biofilms in PBS at the concentrations from 0.6 to 20  $\mu$ M. Equivalent amount of PBS was added into control wells. The cells were incubated for 1 h at 37 °C and stirring at 150 rpm, and then irradiated with a halogen lamp for 15 min with a light dose of 128 J/cm<sup>2</sup>. After irradiation, the wells were washed twice with PBS, and MTT

solution (0.5 mg/mL in PBS) was added and incubated for 1 h at 37 °C. The formed formazan precipitate was dissolved in DMSO with stirring for 30 min. Biofilm destruction was then quantified by measuring the optical density at 492 nm by a microplate reader. The absorbance for the blanks was subtracted from the test values to minimize background interference. The same procedures were performed for non-irradiated control plate.

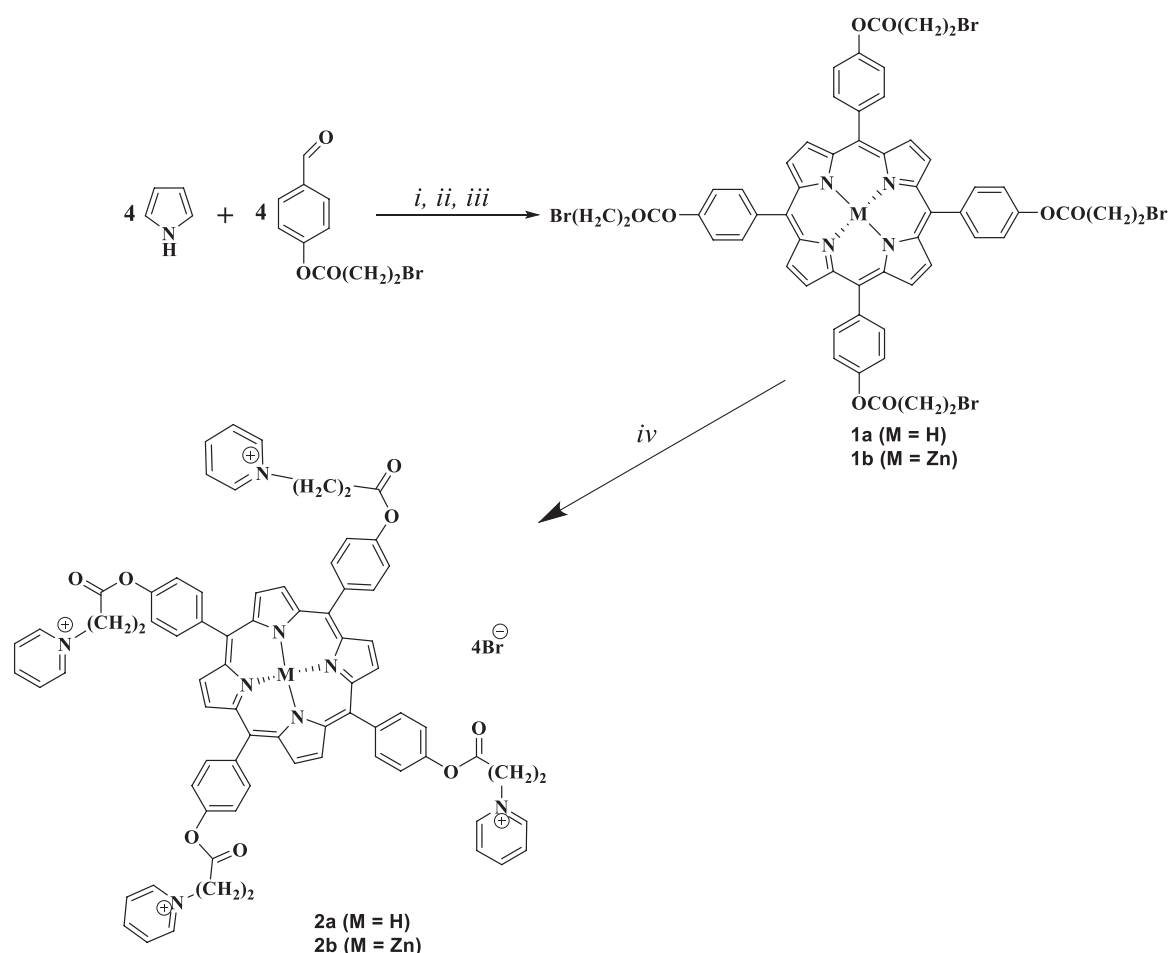
*Statistics.* The results were considered statistically significant with a 95 % confidence level. All experiments were repeated at least 3 times with comparable results. Statistical analysis was performed using the Student's coefficient. Results are presented as mean  $\pm$  SD.

## Results and Discussion

### Synthesis

New cationic *meso*-arylsubstituted porphyrins **2a,b** with charged pyridinium groups were synthesized by the method proposed earlier in our laboratory (Scheme 1).<sup>[28]</sup> At the first stage, functionalized benzaldehyde containing residue of 3-bromopropanoic acid was obtained by acylation of 4-hydroxybenzaldehyde with an acid chloride in the presence of 4-*N,N*-dimethylaminopyridine (DMAP) in 70 % yield.<sup>[29]</sup> The reaction proceeds at low temperature (0 °C) to decrease the formed elimination product and increase the yield. Bromo-substituted porphyrin **1a** was prepared using monopyrrole condensation under mild conditions according to the Lindsey method<sup>[30]</sup> with boron trifluoride etherate (BF<sub>3</sub>OEt<sub>2</sub>) as an acid catalyst. Such approach reduces the number of bromosubstituted porphyrins preparation stages, as well as facilitates their isolation and chromatographic purification. Also, at this stage zinc complex (**1b**) was obtained from compound **1a** in quantitative yield. The preparation of zinc complexes was carried out at the stage of bromo-substituted porphyrins to simplify the isolation by recrystallization and column chromatography. The formation of the metal complex was monitored using EAS. Cationic porphyrins **2a,b** were obtained by the reaction of bromine-substituted precursors quaternization in boiling pyridine, and the target compounds were purified by recrystallization with high yields. The structure of the obtained products was confirmed by multinuclear NMR spectroscopy, UV spectroscopy, mass spectrometry, and elemental analysis. In the <sup>1</sup>H NMR spectra of porphyrins, one narrow signal of  $\beta$ -pyrrole protons was observed at 8.93 ppm, which indicates the presence of a symmetric system in which  $\beta$ -pyrrole protons are equivalent. Signals from aliphatic protons of 3-bromopropanoic acid residues are observed at 3.84 and 3.38 ppm as triplets.

The spectral parameters and photophysical properties of the obtained cationic porphyrins in organic solvents are similar to those for unsubstituted tetraphenylporphyrin (TPP). Peripheral substituents have practically no effect on the electron density distribution in the macrocycle conjugated system. Electronic absorption spectra (EAS) of porphyrins **2a,b** in DMSO and an aqueous Pluronic solution are shown in Figure 1. In the absorption spectra of **2a** five bands are observed: an intense Soret band in the region of 415 nm and four less intense Q-bands (Figure 1); for Zn complexes, EAS display Soret band (428 nm) and two Q-bands (561, 601 nm). Studied compounds belong to the etio-type



**Scheme 1.** Reagents and reaction conditions: *i* –  $\text{BF}_3 \cdot \text{OEt}_2$ ,  $\text{CHCl}_3$ ; *ii* – DDQ; *iii* –  $\text{Zn}(\text{OAc})_2$ ,  $\text{CHCl}_3/\text{CH}_3\text{OH}$ ; *iv* – pyridine, reflux.

with the intensity of the Q bands  $\epsilon_{\text{I}} > \epsilon_{\text{II}} > \epsilon_{\text{III}} > \epsilon_{\text{IV}}$ . The shape of the absorption spectra of compounds **2a,b** is similar in DMSO and aqueous Pluronic F-127 solution (except for a slight hypsochromic shift of **2a,b** absorption maxima caused by a change in the polarity of the medium); however, there is a slight decrease in the extinction coefficient of both compounds in aqueous solution. It can be

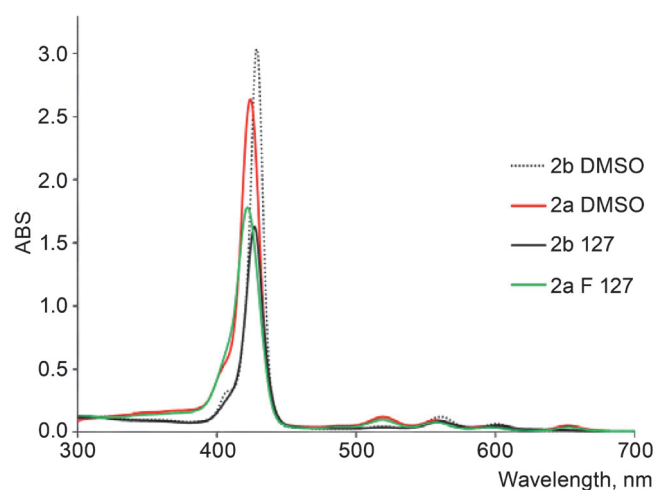


**Figure 1.** EAS of compounds **2a,b** in DMSO and aqueous Pluronic F-127 solution ( $C_{\text{porph}} = 6.5 \mu\text{M}$ ).

explained by an increase in the self-association of molecules in an aqueous polar environment. Summarized data on photophysical parameters are presented in Table 1. The fluorescence spectra of the compounds are shown

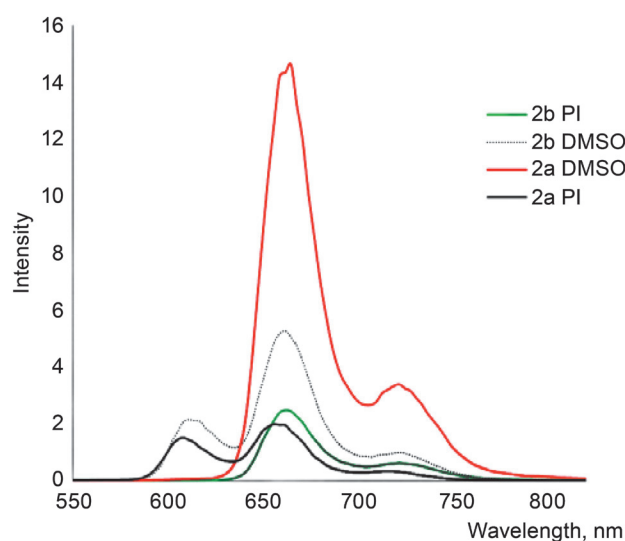


**Figure 2.** Fluorescence spectra of porphyrins **2a,b** in DMSO and aqueous Pluronic F-127 solution ( $C_{\text{porph}} = 6.5 \mu\text{M}$ ,  $\lambda_{\text{ex}} = 430 \text{ nm}$ ).

**Table 1.** Photophysical parameters and partition coefficients of compounds **2a,b**.

	$\lambda_{\text{abs}}$ (nm) ( $\lg \epsilon$ , $\text{mol}^{-1} \cdot \text{cm}^{-1}$ ) <sup>a</sup>					$\lambda_{\text{em}}$ (nm)		$\Phi_F$ <sup>b</sup>	LogP <sup>c</sup>
	Soret	Q <sub>I</sub>	Q <sub>II</sub>	Q <sub>III</sub>	Q <sub>IV</sub>	Q(0,0)	Q(0,1)		
<b>2a</b>	415 (5.49)	512 (4.23)	546 (3.83)	590 (3.56)	645 (3.54)	651	721	0.14	-4.86
<b>2b</b>	418 (5.35)	–	548 (4.15)	592 (3.85)	–	625	672	0.036	-4.6

<sup>a</sup>  $\epsilon$  is an extinction coefficient;

<sup>b</sup> quantum fluorescence yield is determined using TPP in toluene ( $\Phi_F = 0.11$ ) as a standard;

<sup>c</sup> LogP is 1-octanol /water partition coefficient (pH 7) (v/v)

in Figure 2 and Table 1. Upon excitation into the Soret band or any of the Q bands, emission bands were observed in the 600–720 nm region, corresponding to the S<sub>1</sub>→S<sub>0</sub> transition. Fluorescence quantum yields of the studied compounds were determined compared with TPP as a standard (excitation at 513 nm) in toluene. Thus, in a Pluronic solution, a decrease in the fluorescence intensity is observed in comparison with a solution of the monomeric form of PS in DMSO.

### Incorporation of the Porphyrins into Pluronic F-127 Micelles

TPP derivatives are hydrophobic compounds prone to aggregation under physiological conditions. This undesirable phenomenon can be prevented using various delivery vehicles, including Pluronic F-127 polymer micelles. This copolymer is one of the most studied nanoscale carriers for the delivery of PS to cells.<sup>[11,31–32]</sup> Biocompatibility and relatively small size of Pluronic micelles prevent their recognition by the reticuloendothelial system and also increase the circulation time in the bloodstream. The other advantages of this delivery system are the preservation of the fluorescently active monomeric form of porphyrins in solution and a decrease in the probability of nonradiative deactivation of excited states that results in higher fluorescence quantum yield and singlet oxygen generation for solubilized PS. Porphyrin **2a,b** micelles were obtained by the solid dispersion method as described previously.<sup>[33,34]</sup> PS and Pluronic F127 (2.5 %, w/v) were dissolved in methanol, then the mixture was concentrated in vacuum and dried. The result was a thin solid film, soluble in aqueous systems. The resulting micelles were characterized using the dynamic light scattering (DLS). It was found that, in the case of metal-free porphyrin **2a**, the micelles are smaller than the cor-

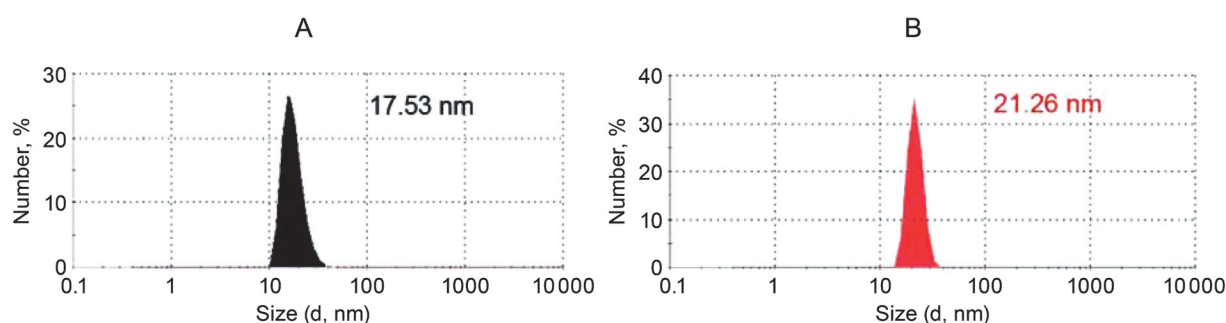
responding Zn(II) complex **2b**. Thus, the particle diameter was 17.53 nm for PS **2a**, and 21.62 nm for **2b** (Figure 3). This may be due to a slight increase in the molecule's hydrophobicity upon the introduction of metal into the macrocycle.<sup>[35]</sup>

### in vitro Biological Tests

The dark and light-induced antibacterial activity of micellar solutions of compounds **2a,b** against a suspension of gram-positive *S. aureus* 209P was studied in the concentration range of 0.6–20  $\mu\text{M}$ . Irradiation was performed with white light (128 J/cm<sup>2</sup>). It was found that free-base porphyrin **2a** inhibits the growth of *S. aureus* bacteria without light irradiation at concentrations higher 5  $\mu\text{M}$ . When irradiated with light, compound **2a** inhibits bacterial growth over the entire studied concentration range (minimum inhibitory concentration < 0.6  $\mu\text{M}$ ) (Figure 4). In contrast, compound **2b** affected weakly bacterial growth at light irradiation (less than 10 %) and did not inhibit it without irradiation in the studied concentration range (Figure 4). Despite the supposedly high photochemical activity of zinc complexes, however, under the conditions of biological tests on *S. aureus* porphyrin **2b** showed antibacterial activity considerably lower than the free-base analogue **2a**. Such effect can be explained by the previously shown increased tendency to self-association for compound **2b** in aqueous media.<sup>[28]</sup> The control solution of Pluronic F-127 did not inhibit bacterial growth.

### Photodynamic Effect on Bacterial Biofilms

The formation of bacterial biofilms leads to an increase in the resistance of bacteria to antimicrobial drugs, and the biofilm itself is a potential source of growth and development of bacteria. In this regard, we also inves-


**Figure 3.** Particle size of micellar solutions of compounds **2a** (A) and **2b** (B), obtained by DLS (concentration 3  $\mu\text{M}$ ).



**Figure 4.** Concentration dependence of dark and light-induced inhibition of *S. aureus* cell growth by compounds **2a,b**.

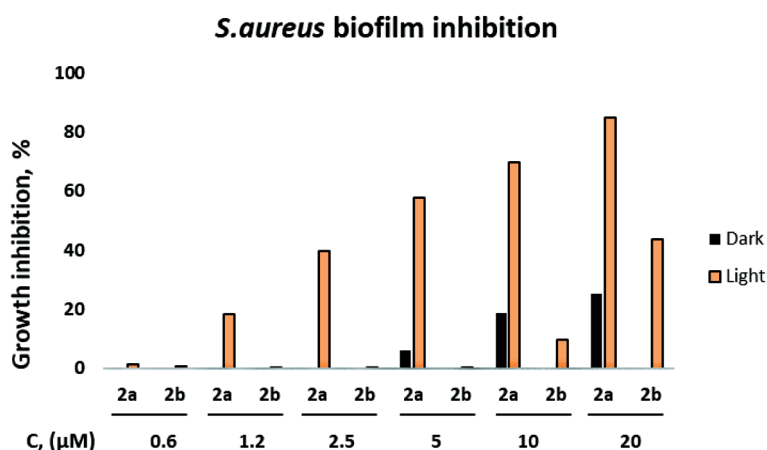


**Figure 5.** Concentration dependence of dark and light-induced toxicity of compounds **2a,b** to *S. aureus* biofilms.

tingated the antibacterial activity of the compounds against the biofilms of bacteria *S. aureus*. It was found that compound **2a** reduces the number of viable bacteria in *S. aureus* biofilms without light irradiation at concentrations higher than 5  $\mu\text{M}$ , and the effect achieves 25 % at 20  $\mu\text{M}$  (Figure 5). Metal complex **2b** and Pluronic F-127 solution do not lead to the death of bacteria in *S. aureus* biofilms without irradiation in the concentration range of 0.6–20  $\mu\text{M}$  (Figure 5). Under irradiation, compounds **2a** and **2b** induce concentration dependent inhibition of bacterial growth in biofilms, and compound **2a** surpasses compound **2b** in this activity. At the 20  $\mu\text{M}$  concentration, photoinduced damage of biofilms achieves 84.8 and 43.5 % for compounds **2a** and **2b**, respectively (Figure 5).

## Conclusions

In the present work, new cationic *meso*-substituted porphyrin **2a** and its complex with Zn(II) (**2b**) were synthesized. The compounds **2a** and **2b** were characterized by physicochemical methods of analysis, their photophysical

properties were studied and a micellar delivery form of **2a** and **2b** was developed with Pluronic F127. *In vitro* experiments on bacterial inactivation revealed that free base **2a** inhibits the growth of gram-positive *S. aureus* in suspension and in biofilms at light irradiation ( $J = 128 \text{ J/cm}^2$ ) in micromolar concentration range. Moderate inhibition of bacterial growth by **2a** was also observed without irradiation. For the zinc complex **2b** inhibition of bacteria in the studied concentration range (0.6–20  $\mu\text{M}$ ) was not achieved.

**Acknowledgements.** This work was financially supported by the Russian Science Foundation (grant No. 20-73-00286).

## References

- Garcia-Alvarez L., Dawson S., Cookson B., Hawkey P. *J. Antimicrob. Chemother.* **2012**, *67*, 137–149.
- Hamblin M.R., Hasan T. *J. Photochem. Photobiol. Sci.* **2004**, *3*, 436–450.
- Wainwright M. *J. Antimicrob. Chemother.* **1998**, *42*, 13–28.
- Kustov A.V., Kustova T.V., Belykh D.V., Khudyaeva I.S., Berezin D.B. *Dyes Pigments* **2020**, *173*, 107948.

5. Lopes L.Q.S., Ramos A.P., Copetti P.M., Acunha T.V., Iglesias B.A., Santos R.C.V., Kolinski-Machado A., Sagrillo M.R. *Microbial Pathogenesis* **2019**, *128*, 47–54.
6. Ezhov A.V., Zhdanova K.A., Bragina N.A., Mironov A.F. *Macroheterocycles* **2016**, *9*, 337–352.
7. Koifman O.I. *et al. Macroheterocycles* **2020**, *13*, 311–467.
8. Lin S., Diercks C.S., Zhang Y.-B., Kornienko N., Nichols E.M., Zhao Y., Paris A.R., Kim D., Yang P., Yaghi O.M., Chang C.J. *Science* **2015**, *349*, 1208–1213.
9. Barona-Castaño J., Carmona-Vargas C., Brocksom T., de Oliveira K. *Molecules* **2016**, *21*, 310.
10. Huang W.-B., Gu W., Huang H.-X., Wang J.-B., Shen W.-X., Lv Y.-Y., Shen J. *Dyes Pigments* **2017**, *143*, 427–435.
11. Bragina N.A., Zhdanova K.A., Mironov A.F. *Russ. Chem. Rev.* **2016**, *85*, 477–512.
12. Pisarek S., Maximova K., Gryko D. *Tetrahedron* **2014**, *70*, 6685.
13. Almeida-Marrero V., González-Delgado J.A., Torres T. *Macroheterocycles* **2019**, *12*, 8–16.
14. Almerie M.Q., Gossedge G., Wright K.E., Jayne D.G. *Photodiagn. Photodyn.* **2017**, *20*, 276–286.
15. Moura N.M.M., Esteves M., Vieira C., Rocha G.M.S.R.O., Amparo M., Faustino F., Almeida A., Cavaleiro J.A.S., Lodeiro C., Neves M.G.P.M.S. *Dyes Pigments* **2019**, *160*, 361–371.
16. Rusakova M.Yu., Ruschak O.V., Vodzinskiy S.V., Ishkov Yu.V. *Macroheterocycles* **2017**, *10*, 289–294.
17. Sengupta D., Timilsina U., Mazumder Z.H., Mukherjee A., Ghimire D., Markandey M., Upadhyaya K., Sharma D., Mishra N., Jha T., Basu S., Gaur R. *Eur. J. Med. Chem.* **2019**, *174*, 66–75.
18. Simões C., Gomes M.C., Neves M.G.P.M.S., Cunha Â., Tomé J.P.C., Tomé A.C., Cavaleiro J.A.S., Almeida A., Faustino M.A.F. *Catal. Today* **2016**, *266*, 197–204.
19. Seeger M.G., Ries A.S., Gressler L.T., Botton S.A., Iglesias B.A., Cargnelutti J.F. *Photodiagn. Photodyn.* **2020**, *32*, 101982.
20. Oniszczyk A., Wojtunik-Kulesza K.A., Oniszczyk T., Kasprzak K. *Biomed. Pharmacother.* **2016**, *83*, 912–929.
21. Gonçalves P.J., Bezzerra F.C., Teles A.V., Menezes L.B., Alves K.M., Alonso L., Alonso A., Andrade M.A., Borissevitch, I.E., Souza G.R.L., Iglesias B.A. *J. Photochem. Photobiol. Chem.* **2020**, *391*, 112375.
22. Managa M., Ngoy B.P., Nyokong T. *J. Photochem. Photobiol. A* **2017**, *339*, 49–58.
23. Lembo A., Tagliatesta P, Guldi D.M. *J. Phys. Chem. A* **2006**, *110*, 11424–11434.
24. Ermilov E.A., Sebastian T., Werncke T., Choi M.T.M., Ng D.K.P., Röder B. *J. Chem. Phys.* **2006**, *328*, 428–437.
25. Gupta I., Ravikanth M. *J. Chem. Sci.* **2005**, *117*, 161–166.
26. Ormond B.A., Freeman S.H. *Dyes Pigments* **2013**, *96*, 440.
27. Amsterdam D. Susceptibility Testing of Antimicrobials in Liquid Media. In: *Antibiotics in Laboratory Medicine*, 4th edition (Loman V., Ed.), Baltimore: Williams and Wilkins; **1996**. pp. 52–111.
28. Zhdanova K.A., Savelyeva I.O., Ignatova A.A., Gradova M.A., Gradov O.V., Lobanov A.V., Feofanov A.V., Mironov A.F., Bragina N.A. *Dyes Pigments* **2020**, *181*, 108561.
29. Fedulova I.N., Bragina N.A., Novikov N.V., Mironov A.F., Bykova V.V., Usol'tseva N.V., Ananieva G.A. *Mendeleev Commun.* **2008**, *18*, 324–326.
30. Lindsey J.S., Hsu H.C., Schreiman I.C. *Tetrahedron Lett.* **1986**, *27*, 4969–4970.
31. Jarak I., Varela C.L., da Silva E.T., Roleira F.F.M., Veiga F., Figueiras A. *Eur. J. Med. Chem.* **2020**, *206*, 112526.
32. Akash M.S.H., Rehman K. *J. Control. Release* **2015**, *209*, 120–138.
33. Managa M., Ngoy B.P., Mafukidze D., Nyokong T. *J. Lumin.* **2018**, *194*, 739–746.
34. Vilsinski B.H., Aparicio J.L., Pereira P.C.S., Fávoro S.L., Campanholi K.S.S, Gerola A.P., Tessaro A.L., Hioka N., Caetano W. *Quim Nova* **2014**, *37*, 1650–1656.
35. Wenceslau A.C., Ferreira G.L.Q.C., Hioka N., Caetano W. *J. Porphyrins Phthalocyanines* **2015**, *19*, 1168–1176.

Received 12.02.2021

Accepted 07.04.2021